New Features in the Catalytic Cycle of Cytochrome P450 during the Formation of Compound I from Compound 0

ARTICLE *in* THE JOURNAL OF PHYSICAL CHEMISTRY B · NOVEMBER 2005

Impact Factor: 3.3 · DOI: 10.1021/jp054754h · Source: PubMed

7 AUTHORS, INCLUDING:

Devesh Kumar
Babasaheb Bhimrao Ambedkar University
101 PUBLICATIONS **4,065** CITATIONS
SEE PROFILE

Sam de Visser
The University of Manchester
178 PUBLICATIONS **7,518** CITATIONS
SEE PROFILE

Jingjing Zheng
Gaussian, Inc.
53 PUBLICATIONS **1,800** CITATIONS
SEE PROFILE

Sason Shaik
Hebrew University of Jerusalem
527 PUBLICATIONS **20,745** CITATIONS
SEE PROFILE

New Features in the Catalytic Cycle of Cytochrome P450 during the Formation of Compound I from Compound 0

Devesh Kumar,[†] Hajime Hirao,[†] Sam P. de Visser,*[,‡] Jingjing Zheng,[§] Dongqi Wang,[§] Walter Thiel,*[,§] and Sason Shaik*[,†]

Department of Organic Chemistry and the Lise Meitner-Minerva Center for Computational Quantum Chemistry, The Hebrew University of Jerusalem, 91904 Jerusalem, Israel, School of Chemical Engineering and Analytical Science, The University of Manchester, Sackville Street, PO Box 88, Manchester M60 1QD, United Kingdom, and The Max-Planck-Institut für Kohlenforschung, Mülheim an der Ruhr, Germany

Received: August 23, 2005

Density functional theory (DFT) is applied to the dark section of the catalytic cycle of the enzyme cytochrome P450, namely, the formation of the active species, Compound I (Cpd I), from the ferric-hydroperoxide species (Cpd 0) by a protonation-assisted mechanism. The chosen 96-atom model includes the key functionalities deduced from experiment: Asp_{251}, Thr_{252}, Glu_{366}, and the water channels that relay the protons. The DFT model calculations show that (a) Cpd I is not formed spontaneously from Cpd 0 by direct protonation, nor is the process very exothermic. The process is virtually thermoneutral and involves a significant barrier such that formation of Cpd I is not facile on this route. (b) Along the protonation pathway, there exists an intermediate, a protonated Cpd 0, which is a potent oxidant since it is a ferric complex of water oxide. Preliminary quantum mechanical/molecular mechanical calculations confirm that Cpd 0 and Cpd I are of similar energy for the chosen model and that protonated Cpd 0 may exist as an unstable intermediate. The paper also addresses the essential role of Thr_{252} as a hydrogen-bond acceptor (in accord with mutation studies of the OH group to OMe).

Introduction

Cytochromes P450 form a class of enzymes that are involved in biosynthesis, detoxification, drug metabolism, brain chemistry, etc.[1] The oxygen insertion reactions catalyzed by these enzymes include C−H hydroxylation, C═C epoxidation, aromatic hydroxylation, heteroatom oxidation, desaturation, and aromatization. This is clearly one of the most versatile and important enzymes in nature.

The species that is believed to perform these reactions is an iron-oxo species, called Compound I (Cpd I, **3** in Scheme 1), which is generated from the precursor species, Compound 0 (Cpd 0, **2**), itself nascent by protonation from the ferric-peroxo species, **1**. While the existence of Cpd I was inferred from transient spectroscopy[2,3] and product analyses,[4−6] it has never been genuinely characterized, although in analogous enzymes such as horseradish peroxidase and chloroperoxidase, the species was isolated and studied in detail.[7,8] Cryogenic X-ray crystallographic characterization[9] of Cpd I of P450 was cast in doubt primarily because EPR/ENDOR studies[4] did not detect the species and showed that it does not accumulate in the cycle even at cryogenic temperatures.

Site-directed mutagenesis studies provided insight into the mechanism of Cpd I formation from the ferric−dioxygen complex. Thus, disruption of the protonation machinery (e.g., of $P450_{cam}$) by mutation of Asp_{251} to Asn (D251N) slowed the appearance of Cpd 0, while replacement of Thr_{252} by Ala (T252A) seemed to terminate the cycle at Cpd 0, although possibly not for all substrates.[10] Moreover, the T252A mutation leads to uncoupling reactions producing hydrogen peroxide rather than Cpd I. As such, the Thr_{252} and Asp_{251} amino acids have emerged as the critical groups involved in the proton relay mechanisms, and their mutations influence the production of side products (uncoupling[1b,c]) at the expense of the formation of Cpd I. Still, however, there are question marks on the existence of Cpd I, the identity of the oxidizing species of P450, and the mechanistic details of Cpd I formation. To tackle this tantalizing problem, we present here a DFT study of the experimentally proposed[11−13] *direct protonation mechanism* that converts Cpd 0 to Cpd I.

SCHEME 1: Formation of Cpd I from Ferric Peroxo (1)

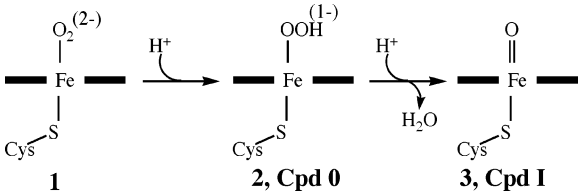

The protonation mechanism in the catalytic cycle of P450 enzymes has been addressed before using DFT. Initial work, by Harris and Loew[14] and Ogliaro et al.[15], used a bare proton to study the species in Scheme 1. In both studies, the process that converts Cpd 0 to Cpd I was found to be spontaneous and highly exothermic (less than −300 kcal/mol).[14,15] Certainly, a spontaneous conversion of Cpd 0 to Cpd I cannot account for the experimental facts[4,10] that Cpd 0 is observed, while Cpd I is not. Indeed, it was recognized by both groups that this minimal model is not realistic and that it was necessary to take

* Corresponding author. Tel.: +972-2-6585909; fax: +972-2-6584680; e-mail: sason@yfaat.ch.huji.ac.il.
[†] The Hebrew University of Jerusalem.
[‡] The University of Manchester.
[§] The Max-Planck-Institut für Kohlenforschung.

10.1021/jp054754h CCC: $30.25
Published on Web 10/04/2005

a more realistic representation of the acid[15] and to account as well for the participation of the water network that acts as a proton shuttle, as done later by Harris (for the first step in Scheme 1).[16] Subsequent DFT calculations of Kamachi and Yoshizawa[17] employed a larger and a more realistic model of $P450_{cam}$, which included side chains of Thr_{252} and Asp_{251} and two crystal waters. Because of the size of the system, a minimal basis set representation of the porphine had to be used, and all heavy atoms were constrained, during geometry optimization, in their positions as in the X-ray structure. The hydroxyl side chain of Thr_{252} was used as the acid that protonates Cpd 0. The study showed that Cpd 0 and Cpd I are close in energy with a small preference of 5.5 kcal mol^{-1} in favor of Cpd I, but no results were reported for the barrier for conversion of Cpd 0 to Cpd I. Subsequently, the process was studied at the QM(DFT)/MM level of theory,[18] using two different QM representations. The small system included, besides the heme, also Thr_{252} and a chain of four water molecules, and it was used for constrained geometry optimization, while the larger system included also Glu_{366} and was used for single-point energy calculations. As in the previous study, here too the hydroxyl side chain of Thr_{252} was taken as the acid that directly protonates Cpd 0 and leads to Cpd I. The conversion of Cpd 0 to Cpd I was found to have a substantial barrier (ca. 14 kcal/mol), but the reaction was calculated to be highly exothermic (−80 kcal/ mol).[18] It is apparent that the two more realistic studies lead to somewhat inconsistent results. Furthermore, neither of the two studies considered the backbone amide group, connecting Thr_{252} to Asp_{251}; this group is thought to have a key role in directing the water channel (that starts from W_{901}).[9] Finally, the use of the hydroxyl side chain of Thr_{252} as the acid that protonates Cpd 0 is enigmatic since experimental data show that the proton of the hydroxyl group is not necessary, as the mutant in which the hydroxyl was changed to a methoxy group produced an active enzyme.[19,20]

In view of the above background, we deemed it timely to reinvestigate the mechanism of conversion of Cpd 0 to Cpd I, with the aim of addressing some of the features observed by experiment.[1b,c,19,20] The study used a large model system, which includes the active species, the experimentally suggested protonation machinery, Thr_{252} and Asp_{251}, and their connecting peptide bond, the second acidic residue Glu_{366},[1b,c,11−13] and the water channel, which appears in the X-ray structure as soon as the heme takes up a dioxygen molecule[9] and that according to solvent kinetic isotope effect studies partakes in the proton shuttle.[1b,c,12] The density functional calculations reported herein reveal a thermoneutral process that has substantial barriers and is mediated by a new intermediate en route to Cpd I.

Methods and Models

Methods. Following previously described procedures,[21−23] we employed the unrestricted hybrid density functional method UB3LYP treatment throughout.[24] All geometries were fully optimized using the Jaguar 5.5 program package followed by an analytical frequency calculation in Gaussian 03;[25,26] all the minima described in this paper have real frequencies only. Initially, we used a modest LACVP(Fe)/6-31G(rest) basis set for the exploratory work, but later all geometries were reoptimized with the LACVP*(Fe)/6-31G*(rest) basis set.[27] Subsequently, single-point calculations using a triple-ζ quality basis set (LACV3P++**(Fe)/6-311++G**(rest)) were performed since this basis set accurately reproduces the proton affinities of the protonating acids within the models.

The effect of the environment on the relative energies of the transition states and the local minima was investigated using the self-consistent reaction field (SCRF) procedure as implemented in Jaguar 5.5.[25] The electronic polarization by medium was mimicked by a dielectric constant of $\epsilon = 5.7$ with a probe radius of 2.72 Å.

TABLE 1: Investigated Models for the Protonation Mechanism

model	A	B	C	D	E
Fe-porphine	+	+	+	+	+
SH axial ligand	+	+	+	+	+
O_2X (X = H, H_2)	*a*	+	+	+	+
Asp_{251}	−	+/−[b]	+	−	+
Thr_{252}	−	+/−[b]	+	+	+
W_{901}	−	+	+	+	+
Glu_{366}[c]	−	−	−	+	+
four crystal waters[d]	−	−	−	+	+
no. of atoms[e]	39−42	73	75	90	96[f]

[a] The distal ligand is variable. [b] Only the side chains of Asp_{251} and Thr_{252} are included. [c] Glu_{366} is represented by acetic acid. [d] The four waters that bridge the carboxylic acid group of Glu_{366} and the hydroxyl group of Thr_{252} (i.e., W_{523}, W_{566}, W_{687}, and W_{902}). [e] Total number of atoms. [f] The peptidic backbone connecting Thr_{252} and Asp_{251} is included.

Model Selection Procedure. To define the most satisfactory system for the proton relay mechanism from Cpd 0 to Cpd I, we gradually tested various models (Table 1), which vary in the size and the available proton sources. This search procedure allowed us to find the minimal model that is able to describe the entire protonation mechanism in the catalytic cycle of P450 enzymes. The smallest system (Model A) is the bare molecule containing iron−porphine with thiolate as an axial ligand and a variable distal ligand. This model was used to calculate the individual species in the catalytic cycle of P450 and identify the spin-state ordering. As expected, it was found[15,28] that with Model A, the protonation is spontaneous and highly exothermic. Thus, since Cpd 0 has been detected experimentally[4,10] these results did not reflect the experiment properly, and an upgrade of the model was necessary.

Models B−E used the geometry of 1DZ8[9] as the starting point with a stepwise addition of parts of the proton delivery system. In Model B, we added to Model A an alcohol−acid pair,[1b,c,9,11−13] an alcohol residue (representing Thr_{252}), and a carboxylic acid group (representing Asp_{251}), and these were augmented by a water molecule (representing W_{901}) that participates in the protonation machinery as suggested by experimental studies[1b,9,11,12] and molecular dynamics (MD) simulations.[29] In Model C, we added the peptide bond between the two amino acid groups Thr_{252} and Asp_{251}. The calculations showed that in Model B, the water molecule (W_{901}) is too mobile due to a missing accepting hydrogen bond from the amide group of the peptide bond,[9] whereas this water molecule is rigid in Model C. Nevertheless, whereas Models B and C led to viable mechanisms for the protonation of the ferric peroxo species (via Asp_{251}−W_{901}) en route to Cpd 0, they both *failed to exhibit a protonation mechanism for Cpd 0 to Cpd I*. As such, we searched for an alternative protonation mechanism using Model D, which contains in addition to the heme−peroxo system (**1**), also Thr_{252}, the side chain of Glu_{366}, and five buried water molecules that form a chain between Thr_{252} and Glu_{366}.[9,11−13] These results showed that Glu_{366} can indeed act as a proton donor[11g,29] that shuttles protons via several water molecules to ferric peroxo species but the conversion stops at Cpd 0 since Thr_{252} is unable to protonate Cpd 0. Thus, both Models C and D produced a mechanism for the protonation of ferric peroxo species leading to Cpd 0 but failed to create a mechanism for the subsequent protonation step leading to Cpd I. Therefore, in agreement with experiment,[19,20] our exploratory work does not support the

previous theoretical results[17,18] that the alcohol group of Thr_{252} can act as a proton donor.

Consequently, it was deemed necessary to combine Models C and D and create the large 96-atom Model E, which includes both proton sources (i.e., the carboxylic acid groups of Asp_{251} and Glu_{366}). This way, Thr_{252} does not act as a proton source but as a relay group in the proton shuttle mechanism.[20] Model E contains the heme system (iron−porphine with thiolate axial ligand and dioxygen as distal ligand) plus the complete amino acids Asp_{251} and Thr_{252} with their peptide bond that holds W_{901} in place, an acetic acid group mimicking the side chain of Glu_{366} plus five crystal water molecules (W_{901}, W_{902}, W_{523}, W_{566}, and W_{687}).[9]

Technical Details on the Chosen Model (Model E). Initially, we ran extensive studies on the complete transformation in Scheme 1 to locate the possible protonation mechanisms from the ferric peroxo species to Cpd I; these studies used the LACVP basis set and fixed the relative positions of a few heavy atoms of the residues relative to the porphyrin. On the basis of these studies, we focused thereafter on the conversion of Cpd 0 to Cpd I in the doublet spin state, using the larger basis set, LACVP*, gradually removing the constraints, and finally fully optimizing all degrees of freedom. The mechanism obtained with LACVP and the constraints was conserved with the larger basis set and the full optimization procedure. We further studied protonation mechanisms from the two acid−alcohol pairs, Asp_{251}−Thr_{252} and Glu_{366}−Thr_{252}, and obtained virtually the same results (that are discussed later). Since an initial step of protonating **1** to give Cpd 0 leaves one of the acids deprotonated, the other acid that remained protonated was used in the second step for the conversion of Cpd 0 to Cpd I. To ascertain that the mechanistic details are not sensitive to the protonation state, we also reoptimized all the critical species, in the presence of the fully protonated acids, that did not affect the conclusions discussed next. Finally, preliminary QM(DFT)/MM results on the same process support the qualitative results from the DFT model study. In view of the enormous amount of computational data produced, we shall only discuss here the results for Model E and present the corresponding numerical data in the Supporting Information. The rest of the material on Models A−D is available from the authors upon request.

Results and Discussion

Our starting point is the structure of Cpd 0, in Figure 1a, obtained by protonation of **1** via the Asp_{251}−W_{901}−Thr_{252} channel, as has been suggested on the basis of experimental data[12,13] and recent MD simulations.[29] This model contains a rotated Asp_{251} residue as originally proposed by Sligar and coworkers.[1b,13] In the crystal structure,[9] Asp_{251} is linked by hydrogen bonding to a charged cluster of Lys_{178}, Asp_{182}, and Arg_{186}, and its rotation will thus require breaking of the salt bridge and other hydrogen bonding interactions, a process that will be facilitated through transient neutralization of Asp_{251} by water from the protein surface.[29] As this specific salt bridge is located near the surface of the enzyme, it is expected that the corresponding arginine side chain quickly abstracts a proton from the solvent. We adopt the working hypothesis[12] that we can use the structure in Figure 1a, with an already rotated Asp_{251}, as a starting point to investigate the mechanism of O−O bond scission in Cpd 0. The model in Figure 1a contains two hydrogen bonding networks, which connect the OOH moiety of Cpd 0 to the carboxylate group of Asp_{251} and to Thr_{252}, as well as the alcohol group of Thr_{252} to the other acidic residue, Glu_{366}, implicated as a potential proton source by experiment[11b,g] and MD simulations.[29]

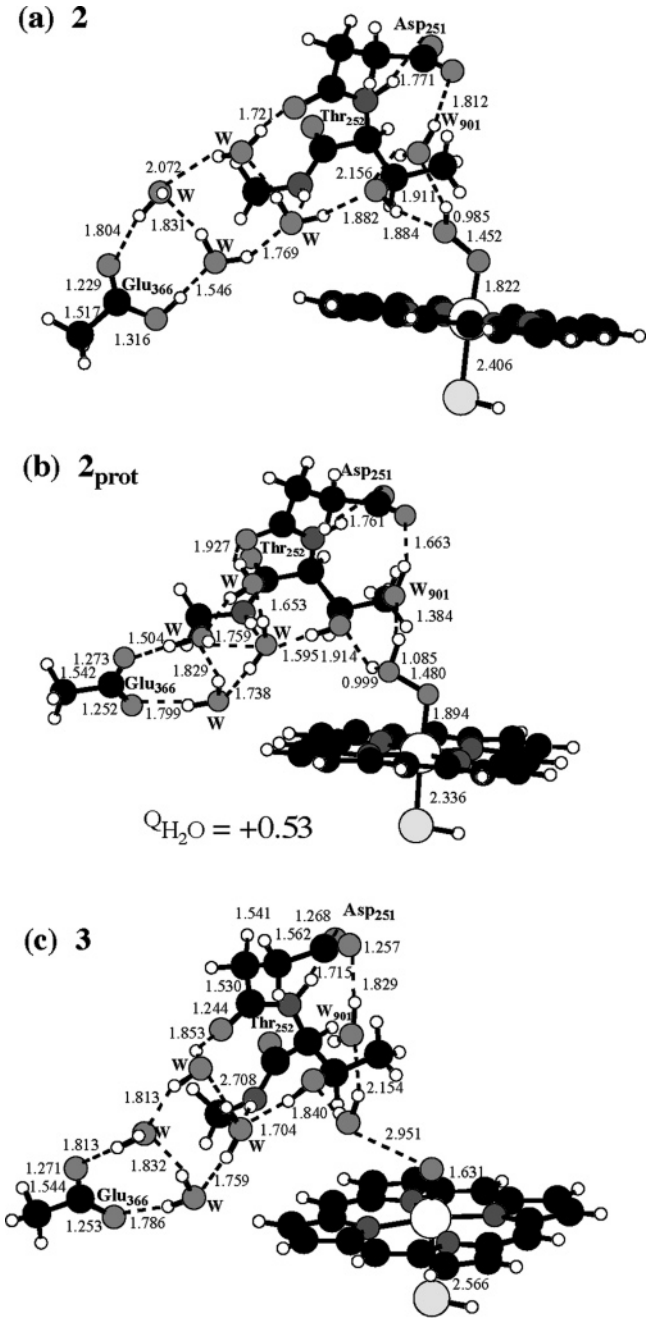

Figure 1. LACVP* fully optimized geometric parameters of Cpd 0, **2** (a), its protonated species, $\mathbf{2}_{prot}$ (b), and Cpd I, **3** (c); all species are in the doublet spin state. In panel b, Q_{H2O} is the Mulliken charge on the water moiety of the $FeO-OH_2$ species.

The Glu−Water−Thr network is set up for a subsequent protonation of Cpd 0 through the Glu_{366} channel. However, as shown in Figure 1b, the protonation does not lead to Cpd I directly but rather to a surprise species, the protonated Cpd 0 ($\mathbf{2}_{prot}$), which is a ferric (Fe^{III}) complex of water−oxide (i.e., $Fe-O-OH_2$). In fact, $\mathbf{2}_{prot}$ is a genuine minimum energy species with both basis sets, LACVP and LACVP*. Notably, enlargement of the basis set shortens the $O-OH_2$ bond of $\mathbf{2}_{prot}$ (from 1.517 Å with LACVP to 1.480 Å with LACVP*). Furthermore, $\mathbf{2}_{prot}$ is also formed when the protonation steps are reversed. In particular, when using a Cpd 0 model with a protonated (i.e., neutral) Asp_{251} carboxylic acid group and a deprotonated Glu_{366} carboxylic acid group, such that Asp_{251} is now the acid that delivers the proton to Cpd 0 rather than to the ferric peroxo (see Figure S14). Finally, the O−O bond in the $\mathbf{2}_{prot}$ system

remains intact upon protonation of the species of Figure 1b at Asp_{251} and subsequent geometry optimization (Figure S14) and also upon protonation of both Asp_{251} and Glu_{366} (Figure S16) and subsequent geometry optimization. Thus, $\mathbf{2}_{prot}$ appears to be a genuine feature of the direct protonation mechanism, for the large model used presently. This species was considered before as a potential intermediate,[14,15,17,18,20,30] but this is the first time it appears as a genuine minimum; all previous theoretical treatments led to the conclusion that the species loses water instantly and collapses into Cpd I in a highly exothermic reaction.

What are the causes of this significant change and the appearance of $\mathbf{2}_{prot}$ in our model? The $O-OH_2$ linkage involves a dative bond[15] from the water molecule to the oxygen atom linked to iron, resulting thereby in a high positive charge on the water moiety ($Q_{H2O} = +0.53$, Figure 1b). Without a proper environment that stabilizes the $(H_2O)^{0.53+}$ moiety that donates electron density to the oxo-iron, the O−O bond would be unstable and fall apart, as found in previous modeling studies.[14−18,30] However, in the present larger model that includes some of the protein neighborhood, the dative bond is stabilized by strong hydrogen bonding of the $(H_2O)^{0.53+}$ moiety to W_{901} and to Thr_{252}, as well as by long-range electrostatic interactions with the negatively charged carboxylate groups of Asp_{251} and Glu_{366}.

The structure of Cpd I is shown in Figure 1c. It is apparent that Thr_{252} plays a key role in the formation of Cpd I by rotating the OH group from its position as a hydrogen bond donor in Cpd 0 (Figure 1a) to a hydrogen bond acceptor that pulls off the water molecule from $\mathbf{2}_{prot}$. However, since the O−O bond of $\mathbf{2}_{prot}$ is persistent, the bond breaking process encounters a barrier. The relative energies of the three species (**2**, $\mathbf{2}_{prot}$, and **3**) are determined by two opposing factors (see more details in the Supporting Information): (i) intrinsically, protonation of the bare Cpd 0 by Glu_{366} (modeled by acetic acid) to yield $\mathbf{2}_{prot}$ is highly endothermic (by 82.6 kcal mol^{-1} with LACV3P++**), and while the subsequent loss of H_2O to yield Cpd I is exothermic, the overall process remains *endothermic* by 17.4 kcal mol^{-1}. (ii) The anionic Cpd 0 is *destabilized* relative to $\mathbf{2}_{prot}$ and Cpd I, presumably by the interactions with the negatively charged Asp_{251}, while $\mathbf{2}_{prot}$ is considerably stabilized, relative to the two other species, by the aforementioned strong hydrogen bonding and long-range interactions (see also Table S7). The net effect is a flattening of the energy landscape, as compared with the bare species: the relative energies of **2**, $\mathbf{2}_{prot}$, and **3** are computed to be 0, 4.49, and 9.11 kcal mol^{-1} using LACVP* and 0, 3.19, and 4.05 kcal mol^{-1} using LACV3P++**. Thus, there is no dramatic basis set effect beyond LACVP*. Incorporating into the LACV3P++** values the ZPE corrections from LACVP* causes minor shifts to 0, 3.22, and 3.28 kcal mol^{-1}. Finally, inclusion of dielectric medium effects (using LACV3P++**) changes the stability order to 0, 10.87, and 0.29 kcal mol^{-1}. Evidently, the more polarizable Cpd I species becomes stabilized by the dielectric medium, but not enough to arrive much below Cpd 0, while $\mathbf{2}_{prot}$ enjoys sufficient stabilization to be a genuine minimum. Significant energy changes relative to the gas phase during protonation are expected in a charged system with polarizable groups. Such energy have been noted before (e.g., by Harris[16]) for the protonation of the ferric−peroxo species, **1**.

The energy profile in Figure 2 depicts some of the computed relative energies and the barriers from LACVP* scans of the direct protonation mechanism. Cpd 0 and Cpd I are of comparable energy but separated by two barriers and the $\mathbf{2}_{prot}$ intermediate. Accordingly, for the adopted conformation of Asp_{251} as suggested by experiment[12,13] (see Figure 1a), the protonation mechanism that converts Cpd 0 to Cpd I is not spontaneous and involves two steps. The $\mathbf{2}_{prot}$ species occurred in all our DFT model calculations, even in the presence of protonated Asp_{251} or/and Glu_{366} (see Figures S14 and S16); the protonation of these acids was found to raise the relative energy of $\mathbf{2}_{prot}$ relative to **2** and **3**, but $\mathbf{2}_{prot}$ remained a genuine minimum.

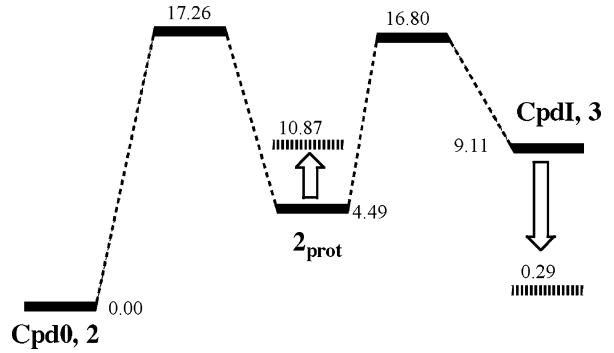

Figure 2. Energy diagram showing relative LACVP* energies of **2**, $\mathbf{2}_{prot}$, and **3** (in doublet spin states); the barriers are estimates from energy scans. The dashed lines show relative energies of $\mathbf{2}_{prot}$ and **3** from LACV3P++** single-point calculations and medium corrections (dielectric constant, $\epsilon = 5.7$), including ZPE correction from LACVP*.

This conclusion was further tested by exploratory quantum mechanical/molecular mechanical (QM/MM) calculations with a QM region that is similar to the present gas-phase model system and is based on the same protonation mechanism (see Supporting Information, Part IV). These QM/MM calculations confirm that Cpd 0 and Cpd I are indeed close in energy, within 5 kcal mol^{-1}, whereas $\mathbf{2}_{prot}$ is considerably less stable, by about 24−33 kcal mol^{-1}. The QM and QM/MM results thus agree that Cpd 0 and Cpd I are close in energy. The energy proximity of Cpd 0 and Cpd I has been noted also in the study of Kamachi and Yoshizawa,[17] who used a system similar to Model C (see Table 1). On the basis of this energy proximity, Cpd I and Cpd 0 might coexist if the reverse barrier for the conversion of Cpd I back to Cpd 0 is not too large as compared with the barrier for substrate oxidation, which of course depends on the substrate. Furthermore, the concentration of Cpd I will depend on fluctuations in its energy relative to Cpd 0, in different protein environments. Another qualitative agreement between the present QM and QM/MM results is the intermediary of $\mathbf{2}_{prot}$ in the direct protonation mechanism. The relative energy of $\mathbf{2}_{prot}$ is sensitive to a number of environmental factors including protonation states and hydrogen bond networks in the protein. Depending on these factors, $\mathbf{2}_{prot}$ may be more or less accessible in the enzyme. Thus, if the direct protonation mechanism is the main process, then the formation of Cpd I from Cpd 0 will neither be facile nor spontaneous. These findings add new facets to the catalytic cycle of P450 and call for more refined studies of the role played by Cpd 0, $\mathbf{2}_{prot}$, and Cpd I.

If indeed, the direct protonation mechanism is the one that converts Cpd 0 to Cpd I, then the present study has some important implications: one is the role of Thr_{252} that acts as a pivot; it donates to and accepts hydrogen bonds from the active center,[1b,12,13] and most importantly, it also assists in the scission of the O−O bond of $\mathbf{2}_{prot}$ to yield Cpd I. Thus, it is not the acidity of Thr_{252} that is important but rather its hydrogen bonding acceptor capability that matters. Indeed, this may be the reason the mutation of the hydroxyl group of Thr_{252} to methoxyl, which retains the hydrogen bond acceptor ability, does not lead to a

loss of catalytic activity of $P450_{cam}$,[19] whereas a mutation like T252A that turns off the ability to accept the hydrogen bond has a detrimental effect on the camphor hydroxylation activity of the enzyme. Furthermore, a recent X-ray structure of the ferrous−dioxygen complex of the T252A mutant shows that the two crystal−water molecules (W_{901} and W_{902} here and W_{235} and W_{453} in ref 20), which are critical for the protonation step, are present also in the mutant. As concluded by Nagano and Poulos,[20] the Thr_{252} residue does not serve as a proton donor but rather as a hydrogen bond acceptor for Cpd 0, whereby it increases the proton affinity of Cpd 0 and assists the O−O cleavage.

Concerning the $\mathbf{2}_{prot}$ intermediate, one would expect a short lifetime and a low concentration on the basis of the computed relative energies. However, since $\mathbf{2}_{prot}$ involves a water oxide molecule coordinated to the Fe^{III} center, it should be a strong oxidant. Given that Cpd 0 is a poor oxidant,[15,31] one may wonder if $\mathbf{2}_{prot}$ could be potentially active in cases where Cpd I cannot form.[32]

Conclusions

We presented here DFT calculations of the direct protonation mechanisms[1b,c,11−13] that convert Cpd 0 of cytochrome P450 (using X-ray data for $P450_{cam}$) to Cpd I, using a carefully crafted model system (Model E, Table 1). Two competing proton sources were identified, originating from either of the acidic residues, Asp_{251} or Glu_{366}, and being shuttled by the water network that connects Glu_{366} to Thr_{252}. Our results show Cpd I is not formed spontaneously but is separated from Cpd 0 by significant barriers and is mediated by the protonated Cpd 0 ($\mathbf{2}_{prot}$). The significant barrier to formation of Cpd I is in accord with the previous[18] and present QM(DFT)/MM results. It is in line with the fact that Cpd 0 enjoys a sufficient lifetime to be detected by experiment.[4,10]

Furthermore, Cpd I and Cpd 0 were found to be very close in energy. On this last point, there is agreement among the present QM(DFT) results, the corresponding results of Kamachi and Yoshizawa,[17] and the preliminary QM(DFT)/MM results mentioned here. Thus, unless the barrier for substrate oxidation by Cpd I is exceedingly small, the coexistence of Cpd I and Cpd 0 cannot be ruled out. This will, however, be highly substrate dependent. We emphasize though that the prediction of the precise relative energies of the two species is not a simple matter since in addition to the effect of the substrate, the relative abundance of the two species will depend on the protein environment and the protonation states of the protein. A more reliable assessment will require extensive QM(DFT)/MM sampling, which is beyond the scope of the present paper.

An important conclusion concerns the role of the alcohol residue Thr_{252}. Our results show that it acts as a hydrogen bond donor acceptor to W_{901}, and to W_{902}, and thereby helps fix the position of these water molecules and sustains a continuous water channel to Glu_{366}. In this indirect manner, Thr_{252} assists W_{901} to accept a hydrogen bond from the OOH moiety of Cpd 0. Subsequently, as $\mathbf{2}_{prot}$ is generated, Thr_{252} acts as a hydrogen bond acceptor to the water moiety of the $FeOOH_2$ unit and helps pull off the water molecule to finally generate Cpd I. Thr_{252} thus plays a pivotal mechanistic role as a relay unit for protonation and hydrogen bonding changes. This role of Thr_{252} is in accord with experimental findings[19,20] that the acidity of this residue does not matter as much as its ability to accept hydrogen bonding.

This intermediate species $\mathbf{2}_{prot}$, having a water oxide moiety, must be a strong oxidant, which might be able to intervene when Cpd I is formed sluggishly as in the T252A mutant.[1b,c] However, it is rather high in energy and has low barriers for conversion into Cpd 0 and Cpd I, so that its mechanistic significance seems questionable under normal circumstances. Further studies are needed to assess its role.

Finally, some qualification is in order: this paper has addressed one particular mechanism of conversion of Cpd 0 to Cpd I, which is deduced from structural, spectroscopic, and mutagenesis data.[1b,c] The conclusions reached are thus restricted to this direct protonation mechanism. Other mechanisms might exist and should be pursued.

Acknowledgment. The research at HU was supported by a grant from BMBF-DIP (Grant DIP-G.7.1) and the Israeli Science Foundation (ISF).

Supporting Information Available: Discussions, tables, and drawings for the Preface, full ref 26, Methods section, LACVP* and LACVP results for model E, and preliminary QM/MM results. This material is available free of charge via the Internet at http://pubs.acs.org.

References and Notes

(1) (a) Ortiz de Montellano, P. R., Ed.; *Cytochrome P450: Structure, Mechanisms, and Biochemistry*, 3rd ed.; Kluwer Academic/Plenum Press: New York, 2005. (b) Makris, T. M.; Denisov, I.; Schlichting, I.; Sligar, S. G. In *Cytochrome P450: Structure, Mechanisms, and Biochemistry*, 3rd ed.; Ortiz de Montellano, P. R., Ed.; Kluwer Academic/Plenum Press: New York, 2005; Ch. 5, p 151. (c) Denisov, I. G.; Makris, T. M.; Sligar, S. G.; Schlichting, I. *Chem. Rev.* **2005**, *105*, 2253−2277.

(2) Egawa, T.; Shimada, H.; Ishimura, Y. *Biophys. Biochem. Res. Commun.* **1994**, *201*, 1464−1469.

(3) Kellner, D. G.; Hung, S. C.; Weiss, K. E.; Sligar, S. G. *J. Biol. Chem.* **2002**, *277*, 9641−9644.

(4) Davydov, R.; Makris, T. M.; Kofman, V.; Werst, D. E.; Sligar, S. G.; Hoffman, B. M. *J. Am. Chem. Soc.* **2001**, *123*, 1403−1415.

(5) He, X.; Ortiz de Montellano, P. R. *J. Biol. Chem.* **2004**, *279*, 39479−39484.

(6) Dowers, T. S.; Rock, D. A.; Jones, J. P. *J. Am. Chem. Soc.* **2004**, *126*, 8868−8869.

(7) Berglund, G. I.; Carlsson, G. H.; Smith, A. T.; Szöke, H.; Henriksen, A.; Hajdu, J. *Nature* **2002**, *417*, 463−468.

(8) Rutter, R.; Hager, L. P.; Dhonau, H.; Hendrich, M.; Valentine, M.; Debrunner, P. *Biochemistry* **1984**, *23*, 6809−6816.

(9) Schlichting, I.; Berendzen, J.; Chu, K.; Stock, A. M.; Maves, S. A.; Benson, D. E.; Sweet, R. M.; Ringe, D.; Petsko, G. A.; Sligar, S. G. *Science* **2000**, *287*, 1615−1622.

(10) Davydov, R.; Perera, R.; Jin, S.; Yang, T.-C.; Bryson, T. A.; Sono, M.; Dawson, J. H.; Hoffmann, B. M. *J. Am. Chem. Soc.* **2005**, *127*, 1403−1413.

(11) (a) Raag, R.; Martinis, S. A.; Sligar, S. G.; Poulos, T. L. *Biochemistry* **1991**, *30*, 11420−11429. (b) Raag, R.; Poulos, T. L. *Biochemistry* **1991**, *30*, 2674−2684. (c) Poulos, T. L.; Finzel, B. C.; Howard, A. J. *Biochemistry* **1986**, *25*, 5314−5322. (d) Cupp-Vickery, J. R.; Poulos, T. L. *Proteins* **1994**, *20*, 197−201. (e) Cupp-Vickery, J. R.; Poulos, T. L. *Nat. Struct. Biol.* **1995**, *2*, 144−153. (f) Cupp-Vickery, J. R.; Han, O.; Hutchinson, C. R.; Poulos, T. L. *Nat. Struct. Biol.* **1996**, *3*, 632−637. (g) Cupp-Vickery, J. R.; Li, H.; Poulos, T. L. In *Cytochrome P450: Structure, Mechanisms, and Biochemistry*, 2nd ed.; Ortiz de Montellano, P. R., Ed.; Plenum Press: New York, 1995; Ch. 4, pp 125−150.

(12) Vidakovic, M.; Sligar, S. G.; Li, H.; Poulos, T. L. *Biochemistry* **1998**, *37*, 9211−9214.

(13) (a) Gerber, N. C.; Sligar, S. G. *J. Am. Chem. Soc.* **1992**, *114*, 8742−8743. (b) Aikens, J.; Sligar, S. G. *J. Am. Chem. Soc.* **1994**, *116*, 1143−1144. (c) Gerber, N. C.; Sligar, S. G. *J. Biol. Chem.* **1994**, *269*, 4260−4266.

(14) Harris, D. L.; Loew, G. H. *J. Am. Chem. Soc.* **1998**, *120*, 8941−8948.

(15) Ogliaro, F.; de Visser, S. P.; Cohen, S.; Sharma, P. K.; Shaik, S. *J. Am. Chem. Soc.* **2002**, *124*, 2806−2817.

(16) Harris, D. L. *J. Inorg. Biochem.* **2002**, *91*, 568−585.

(17) Kamachi, T.; Yoshizawa, K. *J. Am. Chem. Soc.* **2003**, *125*, 4652−4661.

(18) Guallar, V.; Friesner, R. A. *J. Am. Chem. Soc.* **2004**, *126*, 8501−8508.

(19) Kimata, Y.; Shimada, H.; Hirose, T.; Ishimura, Y. *Biochem. Biophys. Res. Commun.* **1995**, *208*, 96−102.
(20) Nagano, S.; Poulos, T. L. *J. Biol. Chem.* **2005**, *280*, 31659−31663.
(21) de Visser, S. P.; Ogliaro, F.; Sharma, P. K.; Shaik, S. *J. Am. Chem. Soc.* **2002**, *124*, 11809−11826.
(22) Kumar, D.; de Visser, S. P.; Sharma, P. K.; Cohen, S.; Shaik, S. *J. Am. Chem. Soc.* **2004**, *126*, 1907−1920.
(23) de Visser, S. P.; Kumar, D.; Cohen, S.; Shacham, R.; Shaik, S. *J. Am. Chem. Soc.* **2004**, *126*, 8362−8363.
(24) (a) Becke, A. D. *J. Chem. Phys.* **1992**, *96*, 2155−2160. (b) Becke, A. D. *J. Chem. Phys.* **1992**, *97*, 9173−9177. (c) Becke, A. D. *J. Chem. Phys.* **1993**, *98*, 5648−5652. (d) Lee, C.; Yang, W.; Parr, R. G. *Phys. Rev. B* **1988**, *37*, 785−789.
(25) *Jaguar 5.5*; Schrödinger, Inc.: Portland, OR, 2000.
(26) Frisch, J. G. et al. *Gaussion 03*; Gaussian, Inc.: Pittsburgh, PA, 2004.
(27) Hay, J. P.; Wadt, W. R. *J. Chem. Phys.* **1985**, *82*, 299−308.
(28) Shaik, S.; Kumar, D.; de Visser, S. P.; Altun, A.; Thiel, W. *Chem. Rev.* **2005**, *105*, 2279−2328.
(29) Taraphder, S.; Hummer, G. *J. Am. Chem. Soc.* **2003**, *125*, 3931−3940.
(30) Loew, G. H.; Harris, D. L. *Chem. Rev.* **2000**, *100*, 407−419.
(31) (a) Sharma, P. K.; de Visser, S. P.; Shaik, S. *J. Am. Chem. Soc.* **2003**, *125*, 8698−8699. (b) Kamachi, T.; Shiota, Y.; Ohta, T.; Yoshizawa, K. *Bull. Chem. Soc. Jpn.* **2003**, *76*, 721−732.
(32) Jin, S.; Makris, T. M.; Bryson, T. A.; Sligar, S. G.; Dawson, J. H. *J. Am. Chem. Soc.* **2003**, *125*, 3406−3407.